THE JOURNAL OF BIOLOGICAL CHEMISTRY
Vol. 274, No. 20, Issue of May 14, pp. 14157–14162, 1999

Printed in U.S.A.

Mitochondria Suppress Local Feedback Activation of Inositol 1,4,5-Trisphosphate Receptors by Ca^{2+}*

(Received for publication, February 25, 1999)

György Hajnóczky‡§, Richard Hager‡, and Andrew P. Thomas‡¶‖

From the ‡Department of Pathology, Anatomy, and Cell Biology, Thomas Jefferson University, Philadelphia, Pennsylvania 19107 and the ¶Department of Pharmacology and Physiology, University of Medicine and Dentistry of New Jersey, New Jersey Medical School, Newark, New Jersey 07103

The concerted action of inositol 1,4,5-trisphosphate (IP_3) and Ca^{2+} on the IP_3 receptor Ca^{2+} release channel (IP_3R) is a fundamental step in the generation of cytosolic Ca^{2+} oscillations and waves, which underlie Ca^{2+} signaling in many cells. Mitochondria appear in close association with regions of endoplasmic reticulum (ER) enriched in IP_3R and are particularly responsive to IP_3-induced increases of cytosolic Ca^{2+} ($[Ca^{2+}]_c$). To determine whether feedback regulation of the IP_3R by released Ca^{2+} is modulated by mitochondrial Ca^{2+} uptake, the interactions between ER and mitochondrial Ca^{2+} pools were examined by fluorescence imaging of compartmentalized Ca^{2+} indicators in permeabilized hepatocytes. IP_3 decreased luminal ER Ca^{2+} ($[Ca^{2+}]_{ER}$), and this was paralleled by an increase in mitochondrial matrix Ca^{2+} ($[Ca^{2+}]_m$) and activation of Ca^{2+}-sensitive mitochondrial metabolism. Remarkably, the decrease in $[Ca^{2+}]_{ER}$ evoked by submaximal IP_3 was enhanced when mitochondrial Ca^{2+} uptake was blocked with ruthenium red or uncoupler. Moreover, subcellular regions that were relatively deficient in mitochondria demonstrated greater sensitivity to IP_3 than regions of the cell with a high density of mitochondria. These data demonstrate that Ca^{2+} uptake by the mitochondria suppresses the local positive feedback effects of Ca^{2+} on the IP_3R, giving rise to subcellular heterogeneity in IP_3 sensitivity and IP_3R excitability. Thus, mitochondria can play an important role in setting the threshold for activation and establishing the subcellular pattern of IP_3-dependent $[Ca^{2+}]_c$ signaling.

The mobilization of intracellular Ca^{2+} stores in response to receptor-stimulated formation of inositol 1,4,5-trisphosphate (IP_3)[1] is dependent on IP_3 receptor Ca^{2+} channels (IP_3R) in the endoplasmic reticulum (ER) (1–4). Both activation and deactivation of the IP_3R is regulated by cytosolic $[Ca^{2+}]$ ($[Ca^{2+}]_c$) (5–9), and this feedback control of IP_3R function by released Ca^{2+} gives rise to the complex spatio-temporal organization of IP_3-induced Ca^{2+} release. Because the regulation of $[Ca^{2+}]_c$ involves a number of other Ca^{2+} transport mechanisms (reviewed in Ref. 10), Ca^{2+} feedback on IP_3R may be modulated by other organelles that transport Ca^{2+}.

Mitochondria are well known to participate in intracellular Ca^{2+} homeostasis, although mitochondrial Ca^{2+} uptake is relatively insensitive to submicromolar increases of $[Ca^{2+}]_c$ (reviewed in Refs. 10 and 11). Rizzuto, Pozzan, and co-workers (12–14) have demonstrated that IP_3R-mediated $[Ca^{2+}]_c$ signals are associated with large increases of mitochondrial matrix $[Ca^{2+}]$ ($[Ca^{2+}]_m$). Furthermore, we have found that IP_3R-mediated $[Ca^{2+}]_c$ oscillations are transmitted into the mitochondria and appear in the form of $[Ca^{2+}]_m$ oscillations (15). The high efficiency of Ca^{2+} signal transmission between the ER and mitochondria is likely to be established by a privileged or local transfer of Ca^{2+} from ER release sites to the mitochondrial Ca^{2+} uptake pathway (12–15). Close associations of ER and mitochondrial membranes (14, 16) and clustering of IP_3R in ER membranes facing mitochondria (17–19) are consistent with such local Ca^{2+} signaling. Although it is also becoming apparent that mitochondria modulate cytosolic Ca^{2+} signaling (20–25), it is not clear whether mitochondria can exert a local control over the feedback effects of IP_3-induced Ca^{2+} release on the IP_3R itself.

In the present study we demonstrate that Ca^{2+} uptake by the mitochondria suppresses the positive feedback effects of Ca^{2+} on the IP_3R in permeabilized hepatocytes. Moreover, our data demonstrate that the mitochondrial modulation of IP_3-induced Ca^{2+} release is limited to those elements of the ER Ca^{2+} stores in proximity with the mitochondria, giving rise to subcellular heterogeneity in IP_3 sensitivity and IP_3R excitability. These properties allow the mitochondria to play a key role in orchestrating the subcellular pattern of $[Ca^{2+}]_c$ signaling.

EXPERIMENTAL PROCEDURES

Hepatocytes plated on polylysine-coated coverslips were maintained in primary culture for 18–24 h (15, 26). Cytosolic $[Ca^{2+}]$ waves in fura2-loaded intact hepatocytes were measured essentially as described previously (15, 27). The cells were stimulated with vasopressin (2–20 nM) prior to and after addition of mitochondrial inhibitors or solvent in sequential runs, and the rate of wave propagation was determined in each condition (15, 27). For permeabilized cell experiments, cells were loaded with fluorescent dyes (obtained from Molecular Probes or Teflabs) by incubation for 30–60 min at 37 °C in medium composed of 121 mM NaCl, 5 mM $NaHCO_3$, 10 mM Na-HEPES, 4.7 mM KCl, 1.2 mM KH_2PO_4, 1.2 mM Mg_2SO_4, 2 mM $CaCl_2$, 10 mM glucose, and 2% bovine serum albumin, pH 7.4, essentially as described previously (9, 15, 26). Dye concentrations were: 150 nM MitoTracker Green, 2 μM rhod2/AM, 5 μM fura2FF/AM, and 5 μM fluo3FF/AM. We have shown previously that compartmentalization of rhod2 occurs in the mitochondria (15) and fura2FF is trapped in the ER (26) of hepatocytes using this loading protocol. Dye-loaded cells were washed with Ca^{2+}-free buffer and then permeabilized by incubation for 6 min with 15 μg/ml digitonin in intracellular medium (ICM) composed of 120 mM KCl, 10 mM NaCl, 1

* This work was supported by Grants DK38422 (to A. P. T.) and DK51526 (to G. H.) from the National Institutes of Health. The costs of publication of this article were defrayed in part by the payment of page charges. This article must therefore be hereby marked "*advertisement*" in accordance with 18 U.S.C. Section 1734 solely to indicate this fact.

§ Recipient of a Burroughs Wellcome Fund Career Award in the Biomedical Sciences.

‖ To whom correspondence should be addressed: Dept. of Pharmacology and Physiology, New Jersey Medical School, UMDNJ, 185 South Orange Ave., University Heights, Newark, NJ 07103. Fax: 973-972-7950; E-mail: thomasap@umdnj.edu.

[1] The abbreviations used are: IP_3, inositol 1,4,5-trisphosphate; IP_3R, IP_3 receptor Ca^{2+} channel; ER, endoplasmic reticulum; $[Ca^{2+}]_c$, cytosolic Ca^{2+}; $[Ca^{2+}]_m$, mitochondrial matrix Ca^{2+}; $[Ca^{2+}]_{ER}$, luminal ER Ca^{2+}; $[Ca^{2+}]_{memb}$, Ca^{2+} at the cytosolic face of intracellular membrane; ICM, intracellular medium; BAPTA, 1,2-bis(o-aminophenoxy)ethane-*N*,*N*,*N*′,*N*′-tetraacetic acid.

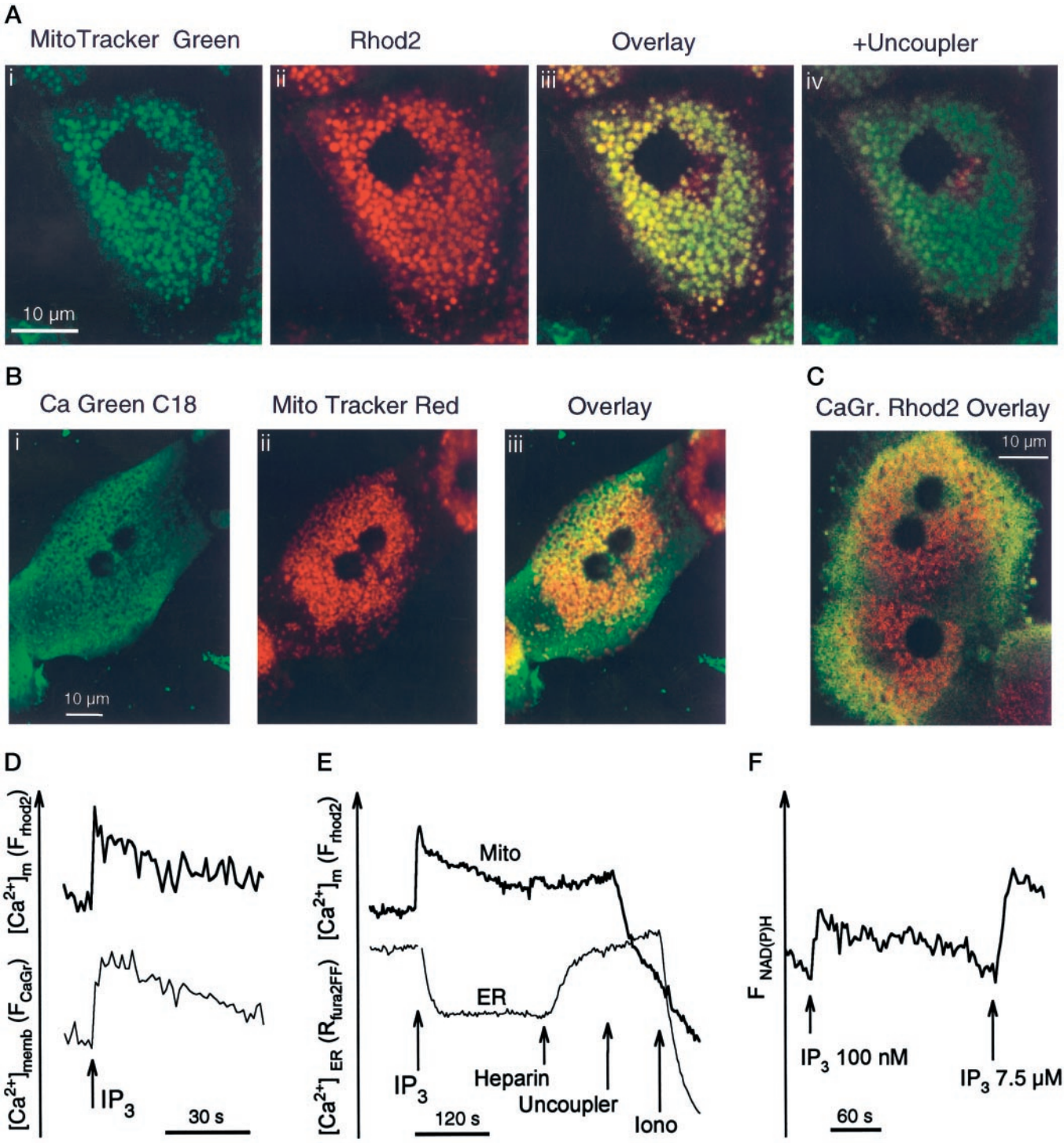

FIG. 1. **IP_3-induced mitochondrial Ca^{2+} uptake in permeabilized hepatocytes.** *A*, localization of mitochondria and measurement of $[Ca^{2+}]_m$ using dual emission confocal imaging of permeabilized hepatocytes loaded with MitoTracker Green and rhod2 (show in *green* and *red*, respectively). These images are overlaid in the *right two panels* to show the coincidence of the labeled organelles (*Overlay*) and the decrease in the rhod2 signal following 5 min of treatment with 5 μg/ml uncoupler 1799 and 5 μg/ml oligomycin (*+Uncoupler*). *B*, dual emission confocal images of CaGreenC18 and MitoTracker red (*left two panels*) and overlay of these images in permeabilized hepatocytes. *C*, overlay image prior to IP_3 addition taken from a dual emission confocal image series using CaGreenC18 (*green*) and rhod2 (*red*) to obtain simultaneous measurements of $[Ca^{2+}]_{memb}$ and $[Ca^{2+}]_m$. *D*, time course of $[Ca^{2+}]_{memb}$ and $[Ca^{2+}]_m$ response to a supramaximal dose of IP_3 (10 μM) recorded from upper cell in *panel C*. *E*, simultaneous measurements of IP_3-induced changes in $[Ca^{2+}]_{ER}$ and $[Ca^{2+}]_m$ using compartmentalized fura2FF and rhod2 in permeabilized hepatocytes. Additions were: 7 μM IP_3, 200 μg/ml heparin, 5 μg/ml 1799 plus 5 μg/ml oligomycin (*Uncoupler*), and 10 μM ionomycin (*Iono*). *F*, effect of IP_3-induced Ca^{2+} mobilization on the redox state of mitochondrial NAD(P)H. The *trace* shows the increases in NAD(P)H fluorescence (360 nm excitation) elicited by sequential additions of 100 nM and 7.5 μM IP_3. Increases of NAD(P)H fluorescence evoked by sequential additions of 100 nM and 7.5 μM IP_3 were 2.9 ± 0.2% ($p < 0.001$) and 5.2 ± 0.4% ($p < 0.025$) in 42 cells. The data are representative of experiments with three or four separate cell preparations.

mM KH_2PO_4, 20 mM Tris-HEPES at pH 7.2 with 2 mM MgATP and 1 μg/ml each of antipain, leupeptin, and pepstatin. ICM was passed through a Chelex column prior to addition of ATP and protease inhibitors to lower the ambient $[Ca^{2+}]$. Labeling of cells with CaGreenC18 (2.5 μM) was carried out during permeabilization. After permeabilization, the cells were washed into fresh buffer without digitonin and

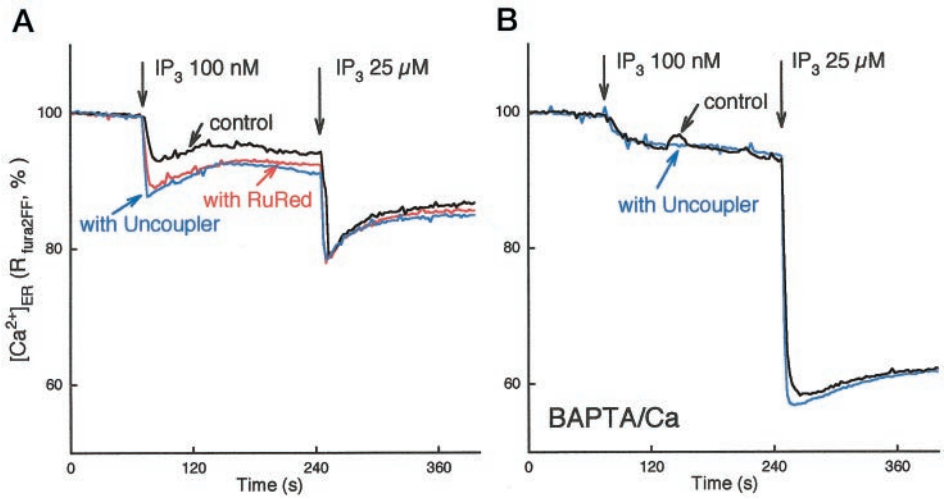

FIG. 2. **Effects of ruthenium red and mitochondrial uncoupling on IP_3-induced decreases of $[Ca^{2+}]_{ER}$.** Fura2FF-loaded hepatocytes were permeabilized and incubated in ICM (*A*) or ICM supplemented with 10 mM BAPTA and 7 mM $CaCl_2$ (*B*), supplemented with 1 μM ruthenium red (*RuRed*, *red trace*), 5 μg/ml uncoupler 1799 plus 5 μg/ml oligomycin (*Uncoupler*, *blue trace*), or no additions (*control*, *black trace*). The $[Ca^{2+}]_{ER}$ decrease in response to sequential treatments with 100 nM and 25 μM IP_3 was then determined. The mean traces are from separate runs using cells from the same preparation and are averaged from the entire cell population in the imaging field (30–50 cells).

incubated in the imaging chamber, at 35 °C. Digital image time series were obtained using a Bio-Rad MRC 600 confocal microscope equipped for dual emission or a Photometrics cooled CCD camera system using a filter wheel and multiwavelength beamsplitter/emission filter combination that allows simultaneous measurement of fura2FF and rhod2 fluorescence. Calibration of fura2FF signals in permeabilized hepatocytes gave values of 300–1000 μM for $[Ca^{2+}]_{ER}$ (K_d = 35 μM, A. Minta, TEFLABS) (26). The fluorescence of rhod2 (F_{rhod2}), CaGreenC18 (F_{CaGr}), and NAD(P)H ($F_{NAD(P)H}$) are expressed as arbitrary units. The fluorescence of rhod2 and CaGreenC18 was not calibrated in terms of absolute $[Ca^{2+}]$, because these are not ratiometric dyes, and photobleaching resulted in a gradual decrease of fluorescence during confocal imaging measurements.

Experiments were carried out with at least three different cell preparations. Traces represent single cell responses unless indicated otherwise. Data are presented as the means ± S.E. Significance of differences from the relevant controls was calculated by Student's *t* test.

RESULTS AND DISCUSSION

In previous studies we have demonstrated that global application of IP_3 to permeabilized hepatocytes results in oscillatory release and reuptake of $[Ca^{2+}]_{ER}$ and that this reproduces the basic mechanism of $[Ca^{2+}]_c$ oscillations in intact cells treated with hormones (26). We have used a similar approach to examine the interactions between mitochondrial and ER Ca^{2+} stores. $[Ca^{2+}]_m$ was monitored with compartmentalized rhod2 (15, 28). Double labeling with the vital mitochondrial dye MitoTracker Green (29) demonstrated that rhod2 fluorescence was completely coincident with the mitochondria in permeabilized hepatocytes (Fig. 1*A*). Moreover, the $[Ca^{2+}]_m$ decrease elicited by uncoupler was manifest in a reduction of rhod2 fluorescence for all of the intracellular structures that were double labeled with MitoTracker (compare overlay *panels iii* and *iv* of Fig. 1*A*), showing that rhod2 selectively monitors $[Ca^{2+}]_m$ in this preparation. To determine whether IP_3-induced Ca^{2+} release led to an increase in $[Ca^{2+}]_m$, we used compartmentalized rhod2 to monitor $[Ca^{2+}]_m$ while simultaneously measuring Ca^{2+} release from the ER. To follow IP_3-induced Ca^{2+} release, $[Ca^{2+}]_{ER}$ was measured with low affinity Ca^{2+} indicators (fura2FF and fluo3FF) as described previously (26). As an alternative approach, Ca^{2+} at the cytosolic face of intracellular membranes ($[Ca^{2+}]_{memb}$) was measured with the lipophilic indicator CaGreenC18 (30). CaGreenC18 labeled membranes throughout the cell, apart from the nuclear matrix, whereas MitoTracker Red fluorescence was predominantly perinuclear, consistent with the subcellular location of mitochondria in these cells (Fig. 1*B*). This differential distribution is also shown in the overlaid CaGreenC18 and rhod2 dual label images of Fig. 1*C*. A similar global distribution of the ER Ca^{2+} stores was observed with fluo3FF or fura2FF, and the perinuclear organization of the mitochondria was also demonstrated based on pyridine nucleotide fluorescence and the alkaline pH of the mitochondrial matrix (see Fig. 3).

Intracellular stores were loaded with Ca^{2+} by incubating the permeabilized cells in the presence of ATP without Ca^{2+} buffers, essentially as described previously (26). Addition of maximal IP_3 to cells loaded with CaGreenC18 and rhod2 resulted in rapid Ca^{2+} release that was detected as an increase in $[Ca^{2+}]_{memb}$ and a simultaneous increase in $[Ca^{2+}]_m$ (Fig. 1*D*). Nevertheless, the CaGreenC18 and rhod2 signals responded differently to uncoupler, which selectively reduced $[Ca^{2+}]_m$ (not shown). The IP_3-induced decrease in $[Ca^{2+}]_{ER}$ could be monitored directly with luminal fura2FF (26), and this was also accompanied by a rapid increase in $[Ca^{2+}]_m$ measured simultaneously with rhod2 (Fig. 1*E*). At the maximal levels of IP_3 used in Fig. 1*E*, the ER remained depleted of Ca^{2+}, but $[Ca^{2+}]_m$ declined after the peak, as reported previously for $[Ca^{2+}]_m$ in intact cells stimulated with a maximal dose of hormone (15). Addition of heparin to block the IP_3 receptor allowed recovery of $[Ca^{2+}]_{ER}$ with essentially no effect on $[Ca^{2+}]_m$, whereas addition of uncoupler to collapse the mitochondrial membrane potential caused $[Ca^{2+}]_m$ to decrease without affecting $[Ca^{2+}]_{ER}$ (Fig. 1*E*). The residual ER Ca^{2+} could be released with ionophore. Several intramitochondrial dehydrogenases are activated by elevated $[Ca^{2+}]_m$ (31), and this activation can be monitored fluorometrically through changes in pyridine nucleotide redox state in intact hepatocytes (15, 32). Fig. 1*F* shows that the IP_3-induced Ca^{2+} release led to an increase in NAD(P)H fluorescence in permeabilized hepatocytes, reflecting the Ca^{2+}-dependent dehydrogenase activation. Taken together, the data of Fig. 1 demonstrate that mitochondrial Ca^{2+} uptake and the consequent regulation of intramitochondrial metabolism is coupled to IP_3-induced Ca^{2+} release from the ER in permeabilized hepatocytes. Because the Ca^{2+} released by IP_3 plays a key role in both positive and negative feedback regulation of the IP_3 receptor Ca^{2+} channel (5–9), we used this system to investigate whether mitochondrial Ca^{2+} uptake modulates IP_3-induced Ca^{2+} release.

The $[Ca^{2+}]_{ER}$ decrease elicited by submaximal and maximal

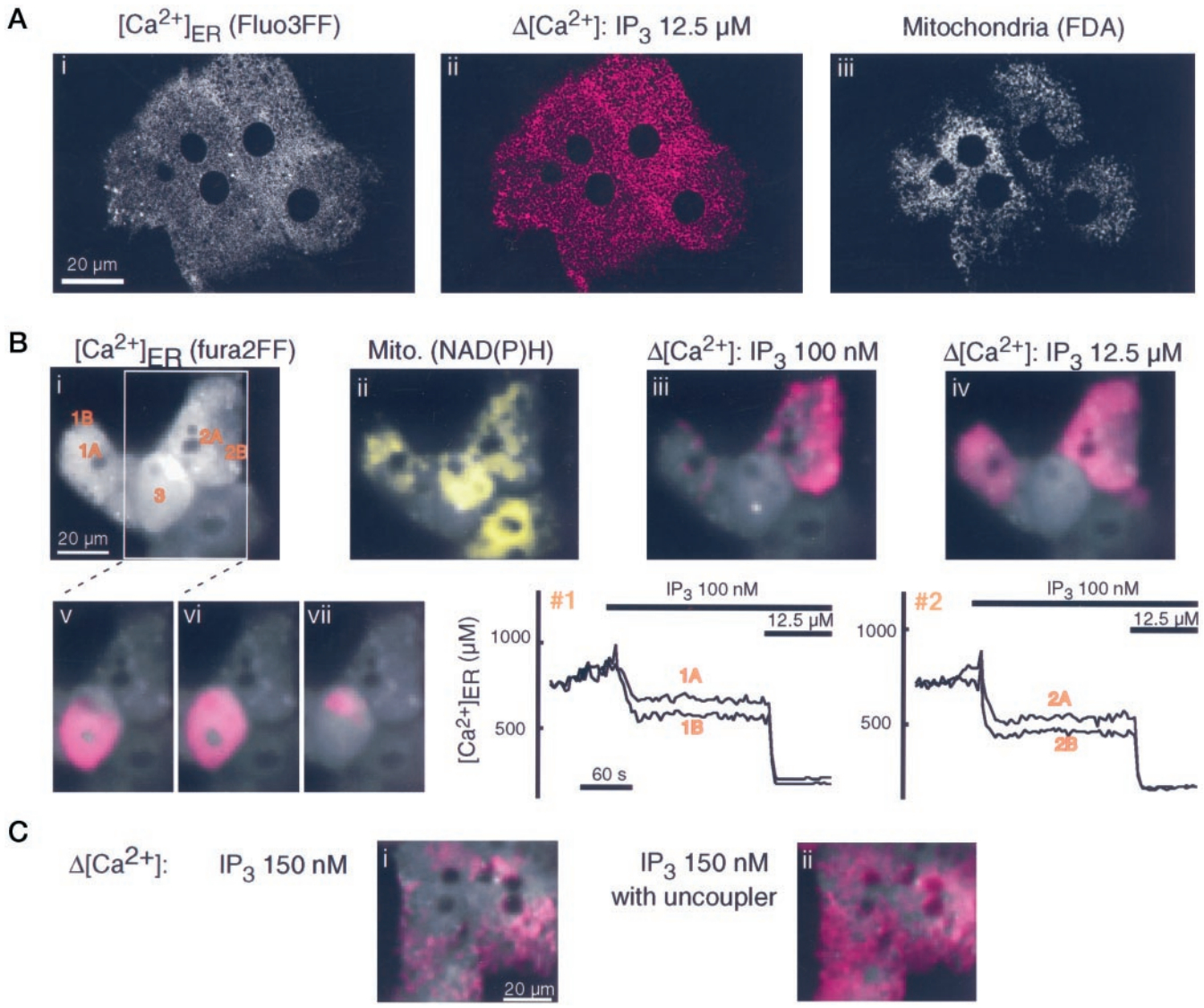

FIG. 3. **Subcellular organization of mitochondrial control over IP_3-induced $[Ca^{2+}]_{ER}$ mobilization.** *A*, the spatial organization of IP_3-sensitive Ca^{2+} stores in individual hepatocytes was determined by confocal imaging measurements of $[Ca^{2+}]_{ER}$ in fluo3FF-loaded permeabilized hepatocytes. *panel i* shows the initial pattern of fluo3FF labeling, and *panel ii* shows the difference image (*purple*) for the effect of 12.5 μM IP_3, calculated by subtraction of the image of IP_3-treated cells from the initial control image. The localization of mitochondria in these cells was determined by subsequent labeling with 150 nM fluorescein diacetate (*panel iii*). *B*, comparison of mitochondrial distribution with the spatial pattern of IP_3-induced $[Ca^{2+}]_{ER}$ decreases. *Gray* scale images show the fluorescence of compartmentalized fura2FF (380 nm excitation) in the permeabilized hepatocytes. The *yellow overlay* of *panel ii* shows the NAD(P)H fluorescence change induced by addition of 20 mM β-hydroxybutyrate. The IP_3-induced increase of $[Ca^{2+}]_m$ had no further effect on NAD(P)H fluorescence after reduction in the presence of β-hydroxybutyrate. Moreover, the NAD(P)H signals canceled out in the ratiometric fura2FF measurements of $[Ca^{2+}]_{ER}$. The *purple overlays* show the fluorescence changes calculated by subtraction of sequential images, giving a differential display of the spatial distribution of IP_3-induced $[Ca^{2+}]_{ER}$ decrease at each time point (15, 26). The cells were treated sequentially with IP_3 concentrations of 100 nM and 12.5 μM. Time courses of $[Ca^{2+}]_{ER}$ change in cells 1 and 2 (*panel i*) for domains with high (*traces 1A* and *2A*) and low (*traces 1B* and *2B*) mitochondrial density are shown below the *upper row* of images. *Panels v–vii* show a time series for the $[Ca^{2+}]_{ER}$ wave recorded in cell 3. *C*, effect of mitochondrial inhibitors on the spatial pattern of IP_3-induced $[Ca^{2+}]_{ER}$ decreases. Responses of $[Ca^{2+}]_{ER}$ to IP_3 (150 nM) were recorded in the absence and presence of FCCP + oligomycin (5 μg/ml each) in sequential runs. To achieve consistent release responses, IP_3 was added together with the Ca^{2+} pump inhibitor cyclopiazonic acid (100 μM), which was washed out between the stimulations. The *purple overlays* show the fluorescence changes calculated by subtraction of the images obtained before and after IP_3 treatment for each condition.

IP_3 was measured under the conditions described above, where the mitochondria were able to take up part of the released Ca^{2+}, and compared with conditions where mitochondrial Ca^{2+}, uptake was blocked with ruthenium red or uncoupler (Fig. 2). These inhibitors affect neither the steady state $[Ca^{2+}]_c$ nor the amount of Ca^{2+} released by IP_3 in liver microsomes, suggesting that they have no direct effect on Ca^{2+} release from ER in hepatocytes (33, 34). Despite the fact that the mitochondrial blockers removed a sink for the released Ca^{2+}, the extent of ER Ca^{2+} release at submaximal IP_3 was actually increased in the presence of ruthenium red or uncoupler (Fig. 2*A*). Under the experimental conditions used in Fig. 2*A*, the Ca^{2+} release response to 100 nM IP_3 was increased from 8.6 ± 1.8% under control conditions to 12.1 ± 1.6% in the presence of ruthenium red ($p < 0.01$, $n = 4$). This did not reflect a change in the size of the releasable ER Ca^{2+} store, because there was no significant difference in the extent of Ca^{2+} release in response to maximal IP_3 (Fig. 2*A*; 25.3 ± 3.5 and 25.1 ± 2.8% in the absence and presence of ruthenium red, respectively; $n = 4$).

We hypothesized that the paradoxical increased efficacy of submaximal IP_3 to release Ca^{2+} when the mitochondria are no longer available to act as a sink for this released Ca^{2+} reflects

the feedback effects of Ca^{2+} on the IP_3R. To examine this possibility, we repeated the experiments of Fig. 2*A* in the presence of BAPTA to clamp $[Ca^{2+}]_c$ at the prestimulation level and prevent local feedback regulation by $[Ca^{2+}]_c$. The $[Ca^{2+}]_{ER}$ decrease in response to submaximal IP_3 was smaller in the presence of BAPTA, presumably because the positive feedback effects of $[Ca^{2+}]_c$ were prevented (Fig. 2*B*). Alternatively, this may be explained by a decrease in IP_3 sensitivity due to the pharmacological effect of BAPTA (35). More importantly, the potentiation by mitochondrial inhibitors at submaximal IP_3 was completely eliminated when the Ca-BAPTA buffer was included. Thus, mitochondrial Ca^{2+} uptake in the immediate vicinity of the IP_3-activated Ca^{2+} release sites can suppress the positive feedback effects of released Ca^{2+} that would otherwise facilitate activation of neighboring IP_3Rs.

The data of Fig. 2 were averaged over a number of cells in the imaging field. However, because mitochondria show a perinuclear distribution in individual hepatocytes, it might be expected that the modulation of IP_3-induced Ca^{2+} release would occur heterogeneously at the subcellular level. The confocal image of Fig. 3*A* (*panel i*) shows that the entire reticular network is labeled with compartmentalized fluo3FF in permeabilized hepatocytes. The decrease of $[Ca^{2+}]_{ER}$ in response to maximal IP_3 occurred homogeneously throughout each cell, apart from the nuclear matrix, as shown by the difference image of Fig. 3*A* (*panel ii*). By contrast, subsequent staining of the mitochondria with the pH-sensitive dye fluorescein diacetate revealed the more centralized mitochondrial distribution (Fig. 3*A*, *panel iii*). Thus, although the IP_3-sensitive Ca^{2+} store appears to be distributed throughout the hepatocyte, the modulation of IP_3 sensitivity by the mitochondria may occur predominately in the central domain of each cell. Evidence in support of this is shown in Fig. 3*B*, where the spatial pattern of $[Ca^{2+}]_{ER}$ decrease evoked by submaximal and maximal IP_3 is compared with the distribution of the mitochondria. Compartmentalized fura2FF was used to monitor $[Ca^{2+}]_{ER}$ (Fig. 3*B*, *panel i*), and the mitochondria were localized functionally by their redox response to the mitochondrial substrate β-hydroxybutyrate (*yellow overlay* in Fig. 3*B*, *panel ii*). The functional mitochondria showed the same perinuclear distribution observed with other techniques in Figs. 1 and 3*A*. Addition of 100 nM IP_3 elicited a partial decrease of $[Ca^{2+}]_{ER}$ (*purple overlays*) in cells 1 and 2, and this response was larger in the peripheral regions than in the central domains where the mitochondria were located (compare *panels ii* and *iii* of Fig. 3*B*). By contrast, subsequent addition of maximal IP_3 elicited a larger decrease in $[Ca^{2+}]_{ER}$ in the mitochondria-rich domains of these cells (Fig. 3*B*, *panel iv*), which primarily reflects the prior depletion of peripheral $[Ca^{2+}]_{ER}$ by the submaximal IP_3 dose. Time courses of $[Ca^{2+}]_{ER}$ change in cells 1 and 2 are shown below the images of Fig. 3*B* (*panels i–iv*) for regions with high mitochondrial density (*traces 1A* and *1B*) and for regions that were relatively deficient in mitochondria (*traces 1B* and *2B*).

Similar differences in IP_3 sensitivity between regions with high and low mitochondrial density were observed in every cell in the imaging field, but because the responses were asynchronous they do not all show in the images. In addition, some cells gave $[Ca^{2+}]_{ER}$ oscillations and waves at submaximal IP_3 (26). For cell 3 of Fig. 3*B*, addition of 100 nM IP_3 did not cause an immediate Ca^{2+} release. Instead, the $[Ca^{2+}]_{ER}$ decrease elicited in cell 2 propagated into cell 3 as a slow wave of Ca^{2+} release (not shown). Significantly, the greatest magnitude and rate of $[Ca^{2+}]_{ER}$ decrease occurred in the distal part of cell 3, which was largely devoid of mitochondria. $[Ca^{2+}]_{ER}$ recovered in this oscillating cell and then after about 90 s in the continuing presence of 100 nM IP_3 there was a second wave of $[Ca^{2+}]_{ER}$ decrease that was intrinsic to cell 3. This intrinsic $[Ca^{2+}]_{ER}$ wave propagated from the mitochondrial-deficient region of the cell (Fig. 3*B*, *panels v–vii*). The suppression of IP_3 sensitivity in subcellular regions that were rich in mitochondria relative to other subcellular regions was observed in all experiments of the type shown in Fig. 3*B*.

To further evaluate the role mitochondrial Ca^{2+} uptake in shaping the subcellular pattern of Ca^{2+} release, the effects of mitochondrial inhibitors on the spatial distribution of $[Ca^{2+}]_{ER}$ decrease induced by IP_3 was examined in the permeabilized cells. Fig. 3*C* shows that the peripherial distribution of $[Ca^{2+}]_{ER}$ decrease observed during the first stimulation with submaximal IP_3 (Fig. 3*C*, *panel i*) was replaced by an essentially uniform response when the same cell was restimulated with the same dose of IP_3 in the presence of mitochondrial uncoupler. Consistent with the idea that mitochondrial Ca^{2+} uptake suppresses IP_3-mediated Ca^{2+} mobilization in intact cells, the rate of propagation of global $[Ca^{2+}]_c$ waves evoked by the IP_3-linked agonist vasopressin in intact hepatocytes was increased by 92 ± 24% ($n = 7$ cells, $p < 0.005$) when the cells were restimulated in the presence of uncoupler (1799+ oligomycin, 5 μg/ml each). By contrast, oligomycin alone had no significant effect on vasopressin-induced $[Ca^{2+}]_c$ waves (27 ± 18% of control, $n = 5$).

Taken together the findings described above demonstrate that the mitochondrial modulation of IP_3-induced Ca^{2+} release is limited to those elements of the ER Ca^{2+} stores in proximity with the mitochondria. As a result, the distribution of mitochondria establishes spatial heterogeneity in IP_3 sensitivity, such that regions lacking mitochondria are most likely to respond first and/or with a greater amplitude of $[Ca^{2+}]_{ER}$ release. Thus, the major finding of the present study is that mitochondrial Ca^{2+} uptake exerts strong control over local Ca^{2+} feedback regulation of IP_3 receptors. This occurs because the mitochondria rapidly sequester a fraction of the released Ca^{2+}, which presumably suppresses the positive feedback effects of this Ca^{2+} on neighboring IP_3 receptors. Because this positive feedback is a key component of the mechanisms responsible for the initiation and propagation of $[Ca^{2+}]_c$ waves, the mitochondria can play a key role in orchestrating the subcellular pattern of $[Ca^{2+}]_c$ signaling.

Mitochondrial Ca^{2+} uptake following IP_3-induced Ca^{2+} release appears to be driven by the relatively large rapid changes in $[Ca^{2+}]_c$ and the privileged access of the mitochondria to IP_3R Ca^{2+} release sites in closely apposed regions of the ER (10–15). We have demonstrated that the $[Ca^{2+}]_c$ oscillations elicited by hormones in intact hepatocytes are coupled to oscillations of $[Ca^{2+}]_m$ (15). These frequency-modulated $[Ca^{2+}]_m$ oscillations establish dynamic control of mitochondrial energy metabolism (15, 32). Although mitochondrial Ca^{2+} uptake clearly serves to transduce $[Ca^{2+}]_c$ signals from the cytosol to regulate Ca^{2+}-dependent processes in the mitochondrial matrix (15, 31), it is also becoming apparent that mitochondria modulate cytosolic Ca^{2+} signaling (20–25). The simplest way in which the mitochondrial Ca^{2+} transport pathways can modify $[Ca^{2+}]_c$ signals is by acting as a slow buffer that accumulates Ca^{2+} during rapid $[Ca^{2+}]_c$ increases and then returns the Ca^{2+} as $[Ca^{2+}]_c$ declines. In this way the mitochondria can blunt and prolong a $[Ca^{2+}]_c$ transient, as occurs during depolarization-induced Ca^{2+} influx in chromaffin cells (22). However, the present study demonstrates that mitochondria can also directly regulate the Ca^{2+} release function of the IP_3R in the ER by modulating the feedback effects of cytosolic Ca^{2+}. This process could account for the observation that mitochondrial energization in *Xenopus* oocytes enhances the organization of IP_3-activated $[Ca^{2+}]_c$ waves by decreasing frequency and increasing the am-

plitude of Ca^{2+} release (20). Specifically, mitochondrial suppression of the positive feedback effects of $[Ca^{2+}]_c$ should reduce the excitability of the system. This stabilization of the basal state would lower Ca^{2+} wave frequency and ensure that a greater proportion of IP_3Rs are in the resting state available to contribute to Ca^{2+} release when the activation threshold is finally achieved at the Ca^{2+} wave front. A different picture has emerged in oligodendrocytes, where mitochondria appear to be selectively localized at sites of Ca^{2+} wave amplification (23, 28). This could reflect a role for mitochondrial Ca^{2+}-induced Ca^{2+} release, whereby the accumulation of $[Ca^{2+}]_m$ elicits mitochondrial depolarization and consequent Ca^{2+} release (24). However, the mechanism described in the present work could also operate in this system, but instead of suppressing positive feedback effects of $[Ca^{2+}]_c$, the spatial and temporal properties of mitochondrial Ca^{2+} uptake in the oligodendrocyte may act predominantly to suppress the negative feedback effects of $[Ca^{2+}]_c$.

Overall, it appears that mitochondria can have a number of important effects on cytosolic Ca^{2+} signaling. These effects are not limited to simple Ca^{2+} buffering but include direct modulation of the feedback effects of $[Ca^{2+}]_c$ on its own release. In addition to shaping the temporal and spatial pattern of $[Ca^{2+}]_c$ transients, the suppression of IP_3 sensitivity by mitochondria may also play a role in stabilizing basal $[Ca^{2+}]_c$. This function of the mitochondria in setting the threshold for $[Ca^{2+}]_c$ spikes, together with the effects on spatial organization and signal amplification can all contribute to enhance the fidelity of Ca^{2+} signaling.

REFERENCES

1. Berridge, M. J. (1993) *Nature* **361,** 315–325
2. Michikawa, T., Miyawaki, A., Furuichi, T., and Mikoshiba, K. (1996) *Crit. Rev. Neurobiol.* **10,** 39–55
3. Clapham, D. E. (1995) *Cell* **80,** 259–268
4. Thomas, A. P., Bird, G. S., Hajnóczky, G., Robb-Gaspers, L. D., and Putney, J. W., Jr. (1996) *FASEB J.* **10,** 1505–1517
5. Iino, M. (1990) *J. Gen. Physiol.* **95,** 1103–1122
6. Finch, E. A., Turner, T. J., and Goldin, S. M. (1991) *Science* **252,** 443–446
7. Bezprozvanny, I., Watras, J., and Ehrlich, B. E. (1991) *Nature* **351,** 751–754
8. Marshall, I. C., and Taylor, C. W. (1993) *J. Biol. Chem.* **268,** 13214–13220
9. Hajnóczky, G., and Thomas, A. P. (1994) *Nature* **370,** 474–477
10. Pozzan, T., Rizzuto, R., Volpe, P., and Meldolesi, J. (1994) *Physiol. Rev.* **74,** 595–636
11. Gunter, T. E., Gunter, K. K., Sheu, S. S., and Gavin. C. E (1994) *Am. J. Physiol.* **267,** C313–C339
12. Rizzuto, R., Brini, M., Murgia, M., and Pozzan, T. (1993) *Science* **262,** 744–747
13. Rizzuto, R., Bastianutto, C., Brini, M., Murgia, M., and Pozzan, T. (1994) *J. Cell Biol.* **126,** 1183–1194
14. Rizzuto, R., Pinton, P., Carrington, W., Fay, F. S., Fogarty, K. E., Lifshitz, L. M., Tuft, R. A., and Pozzan, T. (1998) *Science* **280,** 1763–1766
15. Hajnóczky, G., Robb-Gaspers, L. D., Seitz, M. B., and Thomas, A. P. (1995) *Cell* **82,** 415–424
16. Shore, G. C., and Tata, J. R. (1977) *J. Cell Biol.* **72,** 714–725
17. Maeda, N., Niinobe, M., Inoue, Y., and Mikoshiba, K. (1989) *Dev. Biol.* **133,** 67–76
18. Mignery, G. A., Südhof, T. C., Takei, K., and De Camilli, P. (1989) *Nature* **342,** 192–195
19. Satoh, T., Ross, C. A., Villa, A., Supattapone, S., Pozzan, T., Snyder, S. H., and Meldolesi, J. (1990) *J. Cell Biol.* **111,** 615–624
20. Jouaville, L. S., Ichas, F., Holmuhamedov, E. L., Camacho, P., and Lechleiter, J. D. (1995) *Nature* **377,** 438–441
21. Budd, S. L., and Nicholls, D. G. (1996) *J. Neurochem.* **67,** 2282–2291
22. Babcock, D. F., Herrington, J., Goodwin, P. C., Park, Y. B., and Hille, B. (1997) *J. Cell Biol.* **136,** 833–844
23. Simpson, P. B., Mehotra, S., Lange, G. D., and Russell J. T. (1997) *J. Biol. Chem.* **272,** 22654–22661
24. Ichas, F., Jouaville, L. S., and Mazat, J. P. (1997) *Cell* **89,** 1145–1153
25. Hoth, M., Fanger, C. M., and Lewis, R. S. (1997) *J. Cell Biol.* **137,** 633–648
26. Hajnóczky, G., and Thomas, A. P. (1997) *EMBO J.* **16,** 3533–3543
27. Rooney, T. A., Sass, E. J., and Thomas, A. P. (1990) *J. Biol. Chem.* **18,** 10792–10796
28. Simpson, P. B., and Russell, J. T. (1996) *J. Biol. Chem.* **271,** 33493–33501
29. Haughland, R. P. (1996) *Handbook of Fluorescent Probes and Research Chemicals* (Spence, M. T. Z., ed) pp. 266–271 Molecular Probes Inc., Eugene, OR
30. Tanimura, A., and Turner, R. J. (1996) *J. Biol. Chem.* **271,** 30904–30908
31. McCormack, J. G., Halestrap, A. P., and Denton, R. M. (1990) *Physiol. Rev.* **70,** 391–425
32. Pralong, W. F., Spät, A., and Wollheim, C. B. (1994) *J. Biol. Chem.* **269,** 27310–27314
33. Dawson, A. P., and Irvine, R. F. (1984) *Biochem. Biophys. Res. Commun.* **120,** 858–864
34. Lukács, G. L., Hajnóczky, G., Hunyady, L., and Spät, A., (1987) *Biochim. Biophys. Acta* **931,** 251–254
35. Richardson, A., and Taylor, C. W. (1993) *J. Biol. Chem.* **268,** 11528–11533